A particle resolved approach for simulation of freely evolving sphere suspensions

Ze Cao[1], Danesh K. Tafti[2]

1. Faculty of Infrastructure Engineering
Dalian University of Technology

2. Mechanical Engineering Department
Virginia Polytechnic Institute and State University

Outline

- Motivation
- Particle collision modeling
- Particle Resolved Simulation (PRS) simulations
- Particle dispersion and kinematics analysis

Motivation

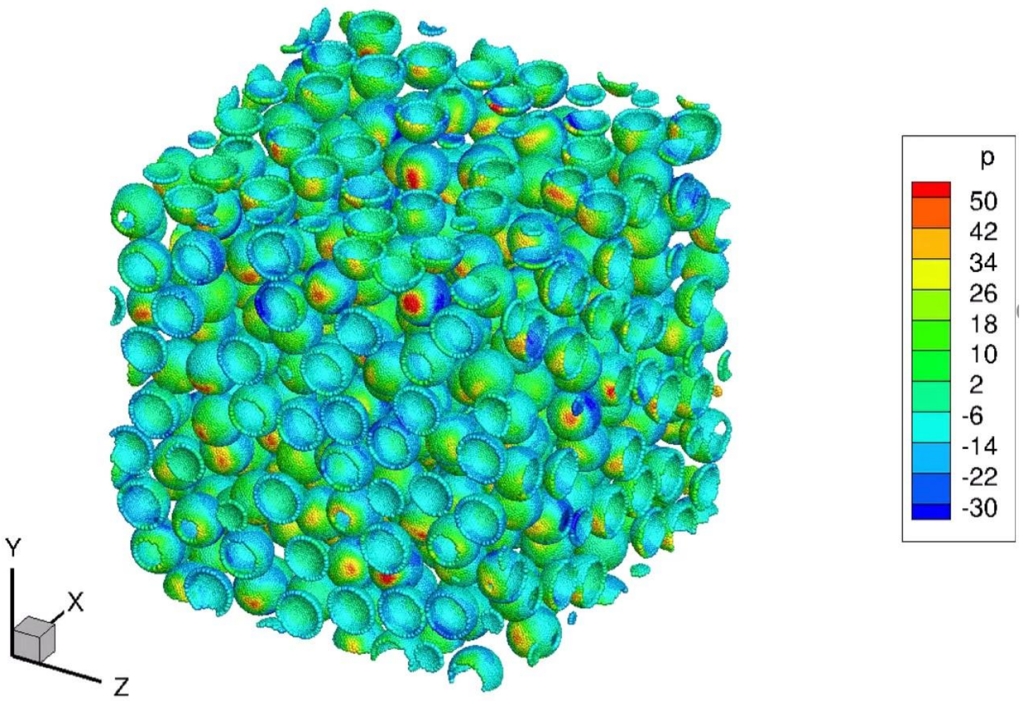

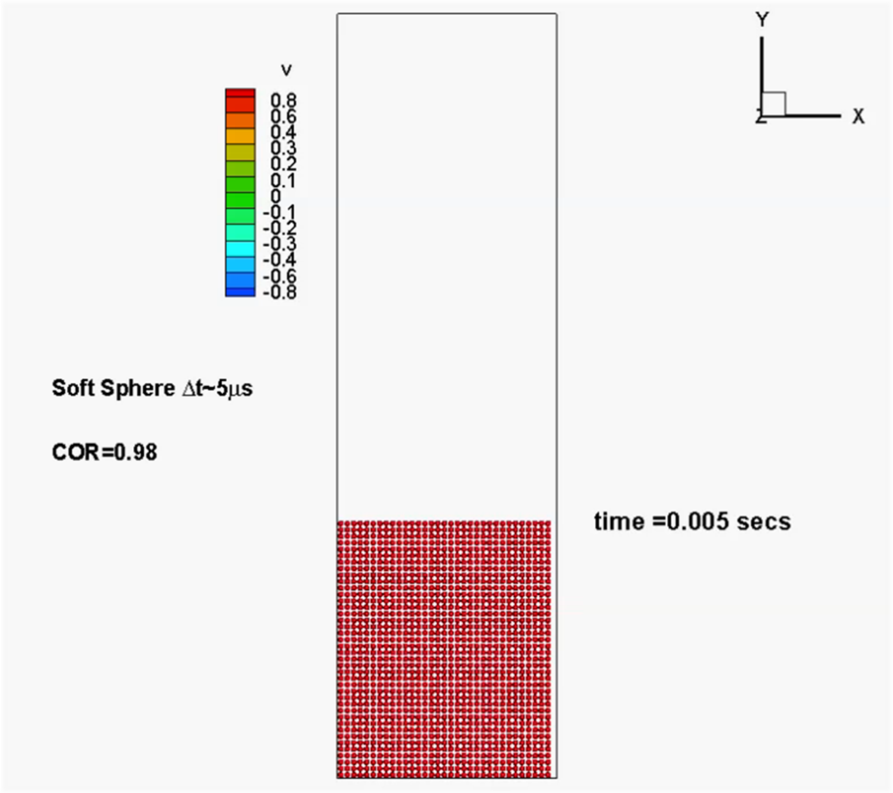

- Development of drag correlations usually from static particle suspensions

- Implementation of drag correlations

Particle collision modeling

- Velocity and pressure from a few layers of fluid node surrounding the immersed surface are interpolated at the solid surface.

- Direct contact leads to probes from one immersed surface embedded in another immersed surface, leading to accuracy and even stability related issues.

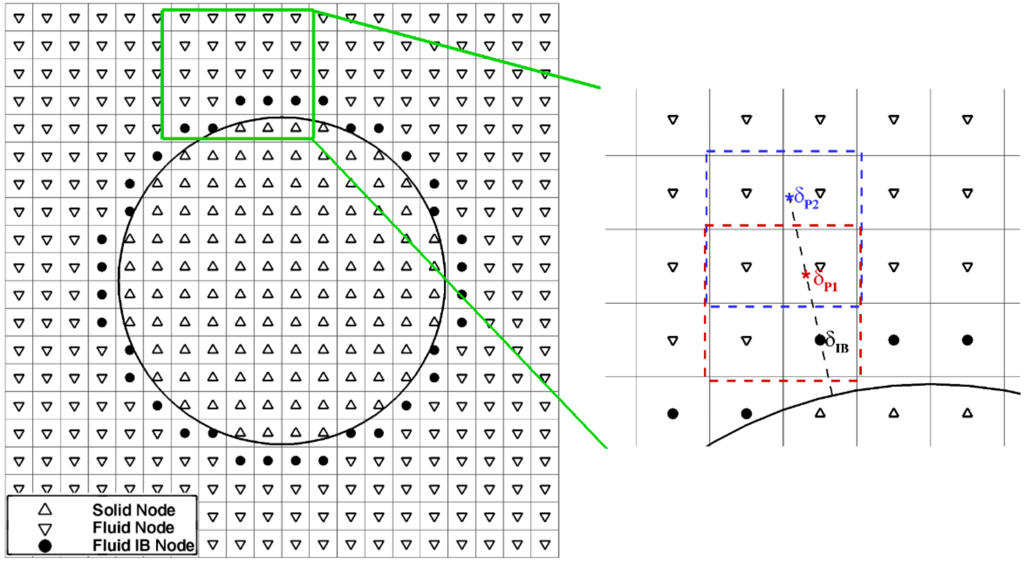

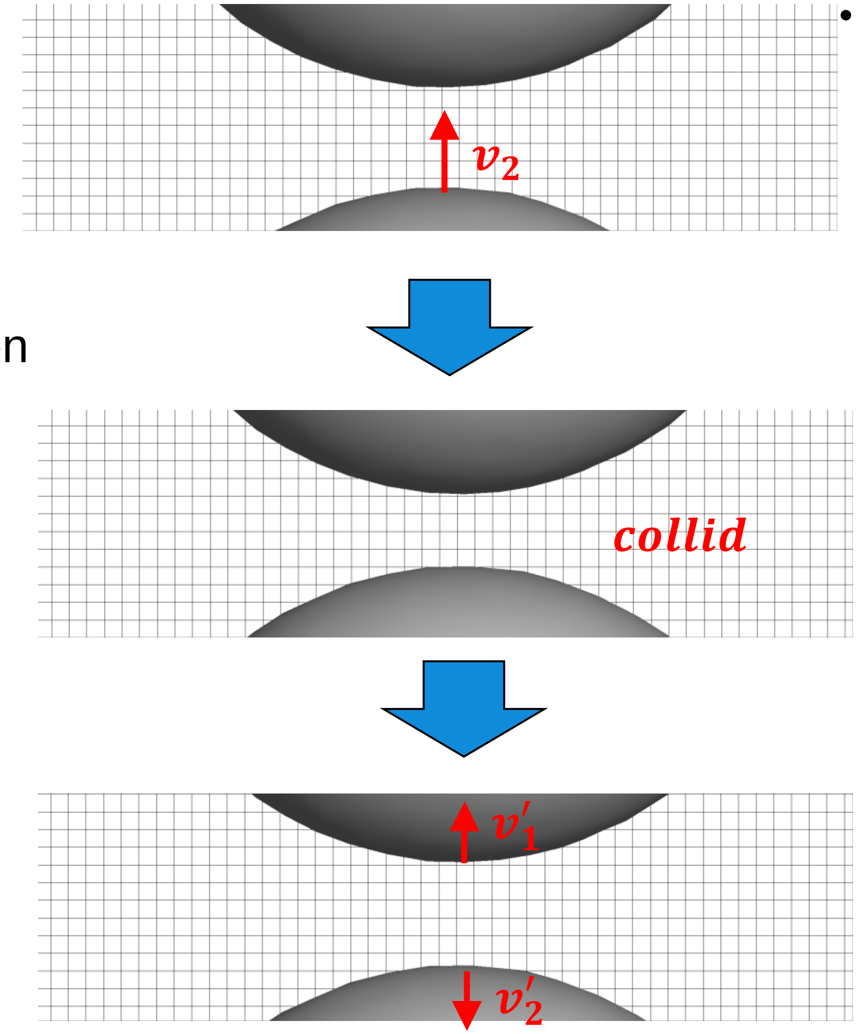

- Before collision, movement of the particles are governed by the force derived from IBM calculation

- Collision are pre-triggered when inter-surface distance diminishes to less than 4 cell edge length.

- Post-collision velocities are derived from soft sphere mode.

Particle collision modeling

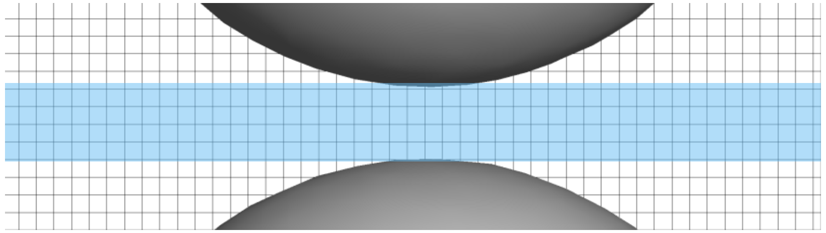

- In reality, lubrication effect arises among two adjacent particles with non-zero relative velocities.
- The lubrication effect behaves like a damper that impedes the particles' relative motion.
- In current simulations, wet coefficient of restitution is adopted to account for lubrication effect:

$$\begin{cases} e_{wet} = \dfrac{u^{*\prime}_{ij,out}}{u^{*\prime}_{ij,in}} \\ e_{wet} = e \cdot \exp(-\dfrac{35}{St}) \\ St = \dfrac{(\rho^*_s + 0.5\rho^*_f)u^{*\prime}_{ij,in} d^*_p}{9\mu^*_{ref}} \end{cases}$$

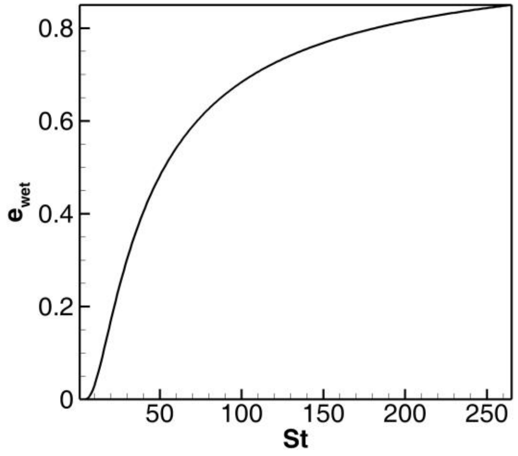

PRS simulations

- Numerical setup

	Grid Resolution	Domain Size	Particle Collision Distance	Re	φ	Symbol Type
Base setup	$\frac{1}{40}d_p$	$5d_p \times 5d_p \times 5d_p$	$0.1d_p$	10, 50, 100, 200, 300	0.1, 0.2, 0.3, 0.4	○
Setup 1	$\frac{1}{40}d_p$	$9d_p \times 9d_p \times 9d_p$	$0.1d_p$	10, 50, 100, 200, 300	0.1, 0.2, 0.3, 0.4	△
Setup 2	$\frac{1}{80}d_p$	$5d_p \times 5d_p \times 5d_p$	$0.05d_p$	10, 50, 100, 200, 300	0.1, 0.3, 0.4	▽

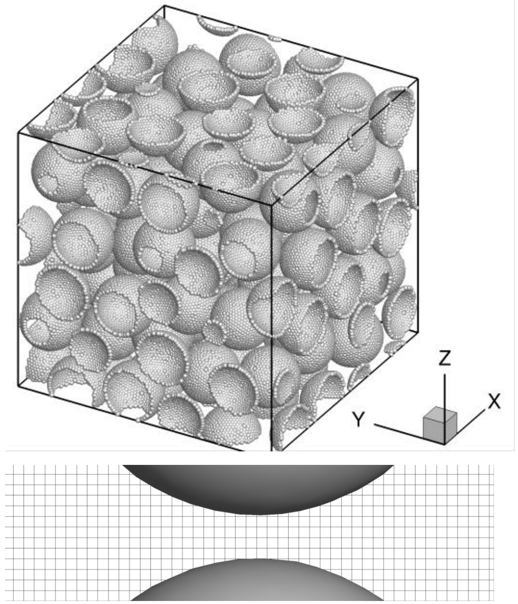

Base case

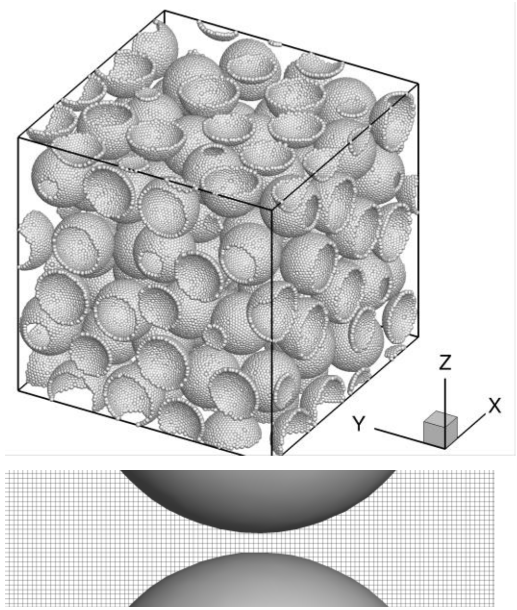

Setup 1

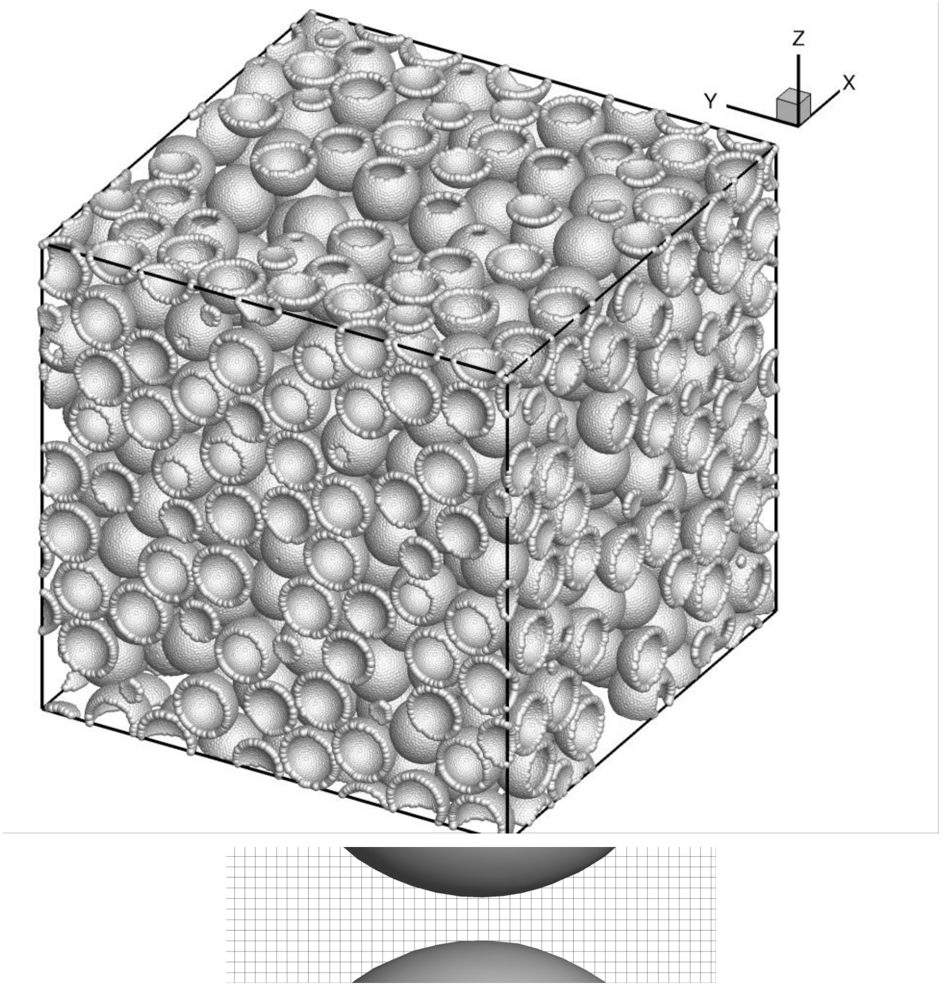

Setup 2

PRS results (static suspension)

- Static suspension results and comparison

Author	Drag correlation	Applicability
Rong et al. (2013)	$F_d = \frac{10\varphi}{(1-\varphi)^2} + (1-\varphi)^2\left(1+1.5\sqrt{\varphi}\right) + (0.11\varphi(1+\varphi) - \frac{0.00456}{(1-\varphi)^4} + (0.169(1-\varphi)^2 + \frac{0.0644}{(1-\varphi)^4}))Re^{-0.343})Re$	$50 \leq Re \leq 1000$, $0.1 \leq \varphi \leq 0.6$, Spherical particle suspensions.
Tenneti et al. (2011)	$F(\varphi, Re) = \frac{F_{iso}}{(1-\varphi)^3} + F_\varphi(\varphi) + F_{\varphi,Re}(\varphi, Re)$, $F_\varphi(\varphi) = \frac{5.81\varphi}{(1-\varphi)^3} + 0.48\frac{\varphi^{1/3}}{(1-\varphi)^4}$, $F_{\varphi,Re}(\varphi, Re) = \varphi^3 Re(0.95 + \frac{0.61\varphi^3}{(1-\varphi)^2})$.	$0.01 \leq Re \leq 300$, $0.1 \leq \varphi \leq 0.5$, Spherical particle suspensions.

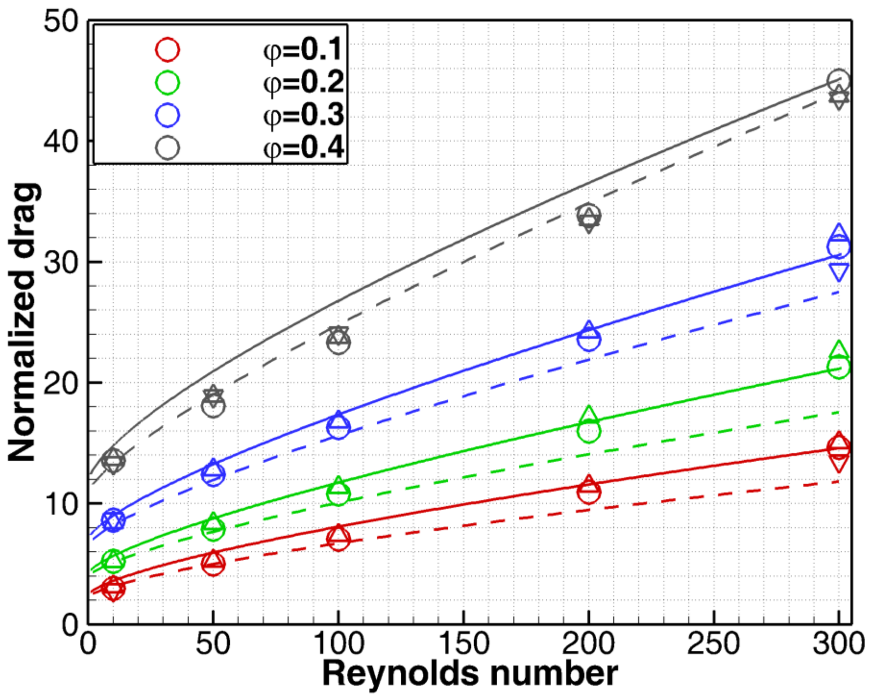

Solid lines: Correlation of Tang et al.
Dashed lines: Correlation of Tenneti et al.

PRS results (free evolving suspension)

- One case with Re=50, $\varphi = 0.3$

- Movement of particles
- X-directional flow velocity

PRS results (free evolving suspension)

- Freely evolving suspension with different solid-fluid density ratios

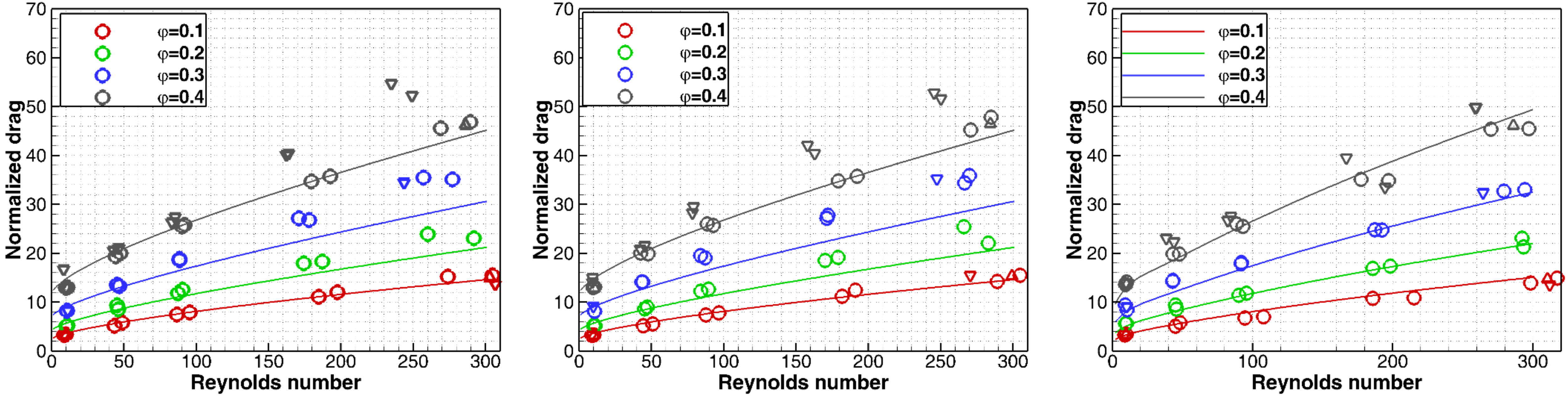

$\frac{\rho_s}{\rho_f} = 2$ $\frac{\rho_s}{\rho_f} = 10$ $\frac{\rho_s}{\rho_f} = 100$

PRS results (free evolving suspension)

- Movable suspension drag correlations

Author	Drag force correlation	Applicability
Tavanashad et al.	$F_d = F_{iso} \cdot (78.96\varphi^3 - 18.63\varphi^2 + 9.845\varphi + 1)^n$ $F_{iso} = 1 + 0.15Re^{0.687}$ $\begin{cases} n = 1, & \rho_s/\rho_f \leq 10 \\ \dfrac{1.05 - n}{n = 0.9} = 4.3 \times 10^{-4} Re^{2.361} & \rho_s/\rho_f = 100 \end{cases}$	$10 \leq Re \leq 100$ $0.1 \leq \varphi \leq 0.4$ $0.01 \leq \rho_s/\rho_f \leq 100$
Tang et al.	$F_d = F_{stat} \cdot Re_T \cdot \dfrac{\varphi}{(1-\varphi)^2}$	$40 \leq Re \leq 1000$ $0.1 \leq \varphi \leq 0.45$ $500 \leq \rho_s/\rho_f \leq 3000$
Huang et al.	$F_d = F_{stat} + 4.01 \dfrac{(1.93\varphi^2 + 0.25\varphi + 0.66)}{(1-\varphi)^{0.1}} \cdot \dfrac{Re_T^{1.49}}{Re^{0.8} + 100}$	$5 \leq Re \leq 120$ $0.1 \leq \varphi \leq 0.6$ $Re_T \leq 34.6$

- Tavanashad and Tang performed their simulations for freely evolving sphere suspensions.
- Huang assigned random velocities that obeyed the isotropic Maxwellian distribution to the particles in the suspension mimicking the effect of particle movement in freely evolving suspensions

PRS results (free evolving suspension)

- Movable suspension drag correlations
- Results at sold volume fraction between 0.1 and 0.3

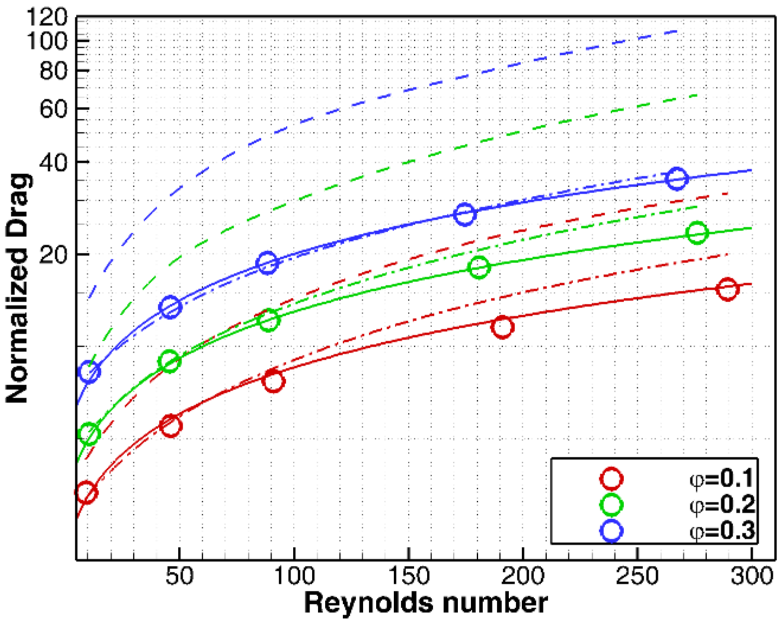

$$\frac{\rho_s}{\rho_f} = 2$$

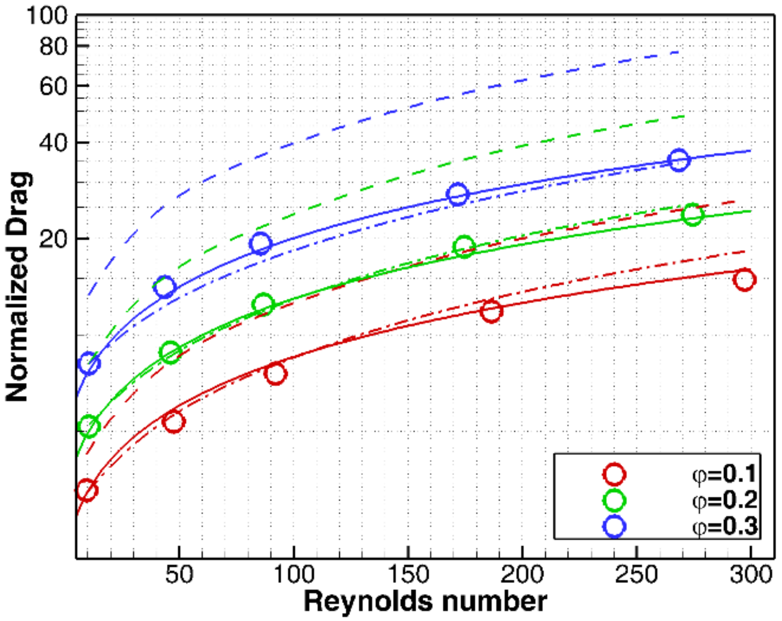

$$\frac{\rho_s}{\rho_f} = 10$$

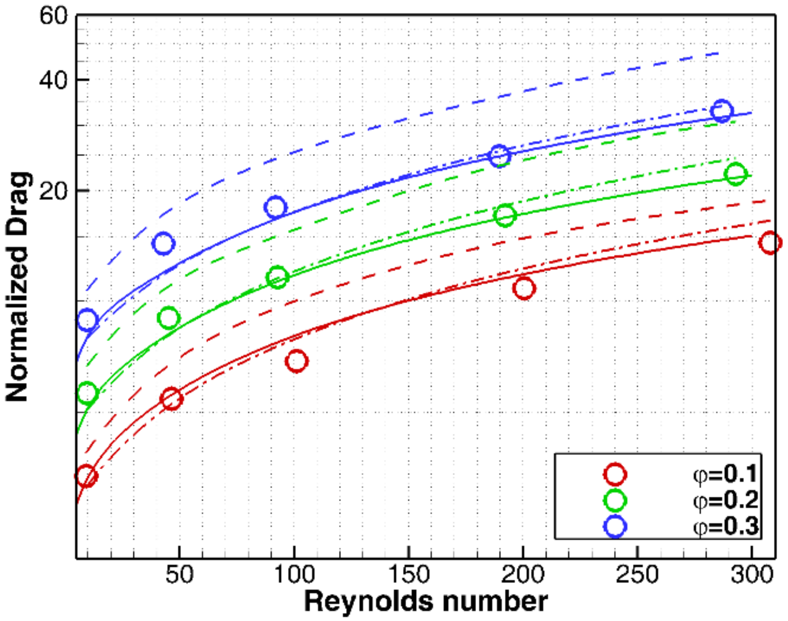

$$\frac{\rho_s}{\rho_f} = 100$$

Solid lines: Tavanashad's correlation;
dashed lines: Tang's correlation;
dash dot lines: Huang's correlation

PRS results (free evolving suspension)

- Movable suspension drag correlations
- Results at solid volume fraction of 0.4

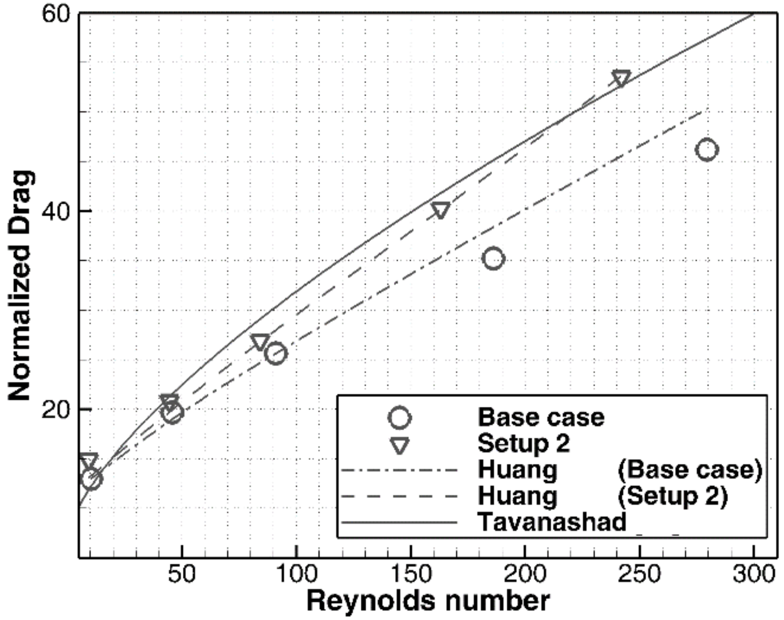

$$\frac{\rho_s}{\rho_f} = 2$$

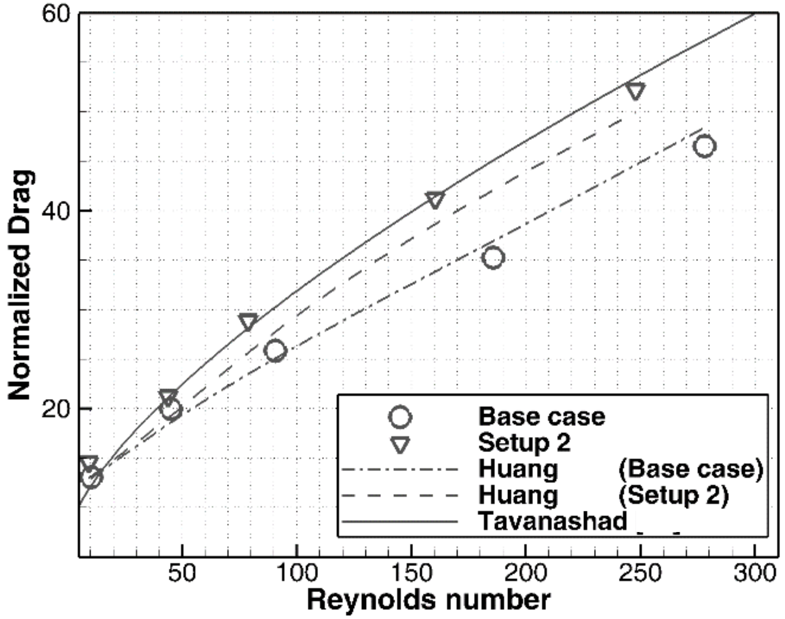

$$\frac{\rho_s}{\rho_f} = 10$$

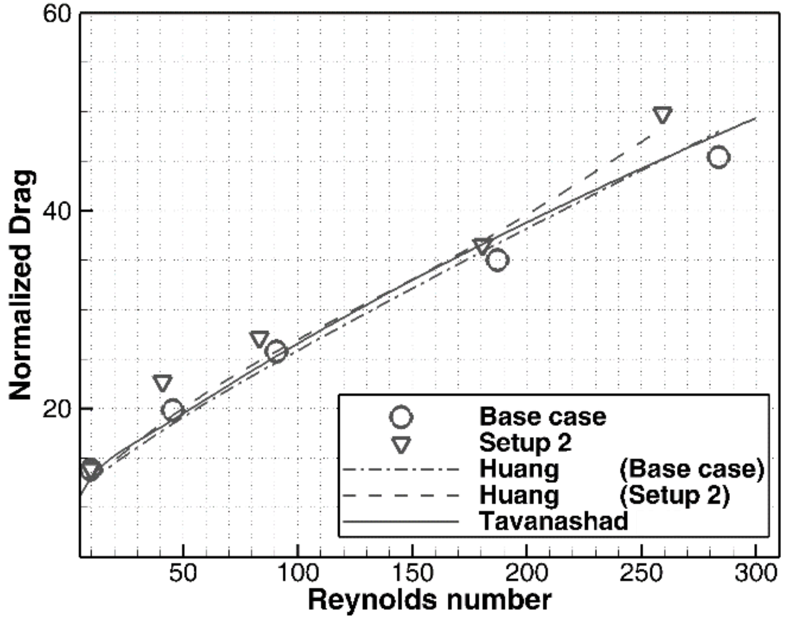

$$\frac{\rho_s}{\rho_f} = 100$$

Solid lines: Tavanashad's correlation;
dashed lines: Tang's correlation;
dash dot lines: Huang's correlation

Particle dispersion

- Radial Distribution Function (RDF) in sphere suspensions at $\varphi = 0.4$

$$g(r) = \frac{2V_{sys}}{N(N-1)}\frac{1}{V_r}\sum_{i=1}^{N}\sum_{j=1,i\neq j}^{N}\theta(r_{ij}-r)\theta(r+\Delta r-r_{ij}),$$

$$\theta(r') = \begin{cases}1, & r' > 0\\ 0, & r' \leq 0\end{cases}.$$

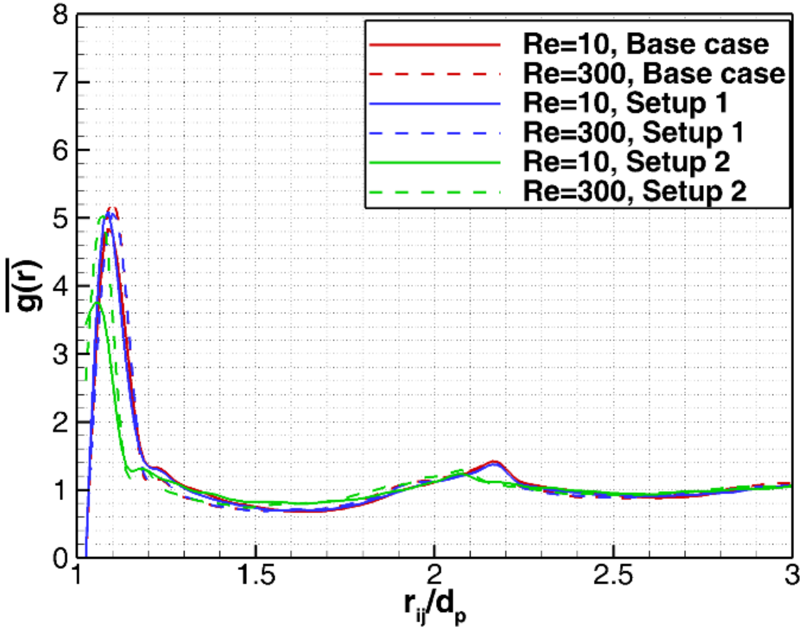

$\frac{\rho_s}{\rho_f} = 2$

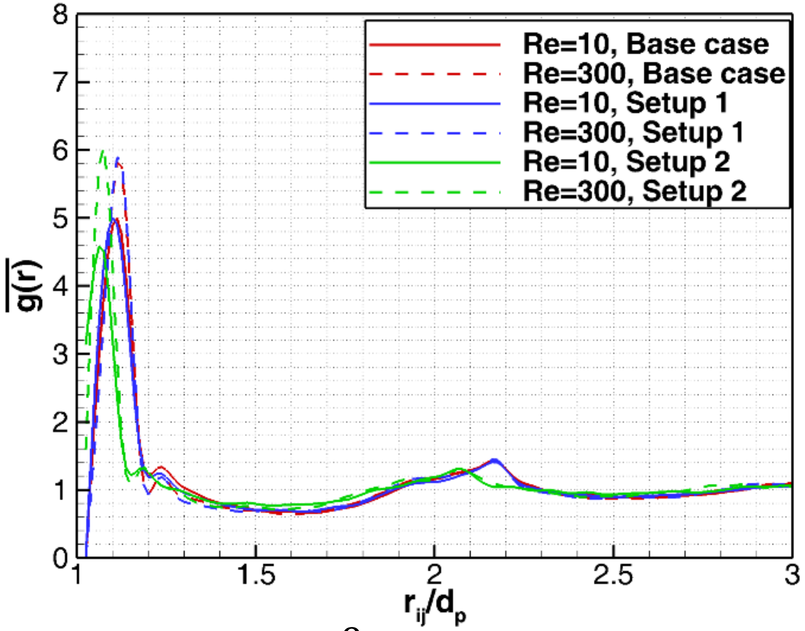

$\frac{\rho_s}{\rho_f} = 10$

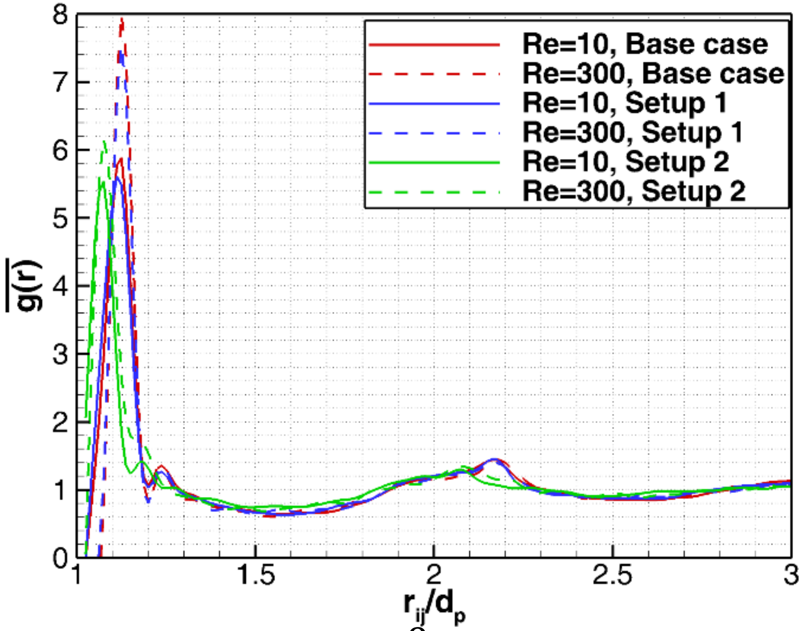

$\frac{\rho_s}{\rho_f} = 100$

- Different numerical setups don’t make significant difference in the particle dispersion in freely evolving suspensions

Particle kinematics analysis

- Granular temperature in the particle suspensions

$$T^* = \frac{1}{3N}\sum_{k=x,y,z}\sum_{i=1}^{N}\left(v_{i,k}^* - v_k^*\right)^2,$$

$$Re_T = \frac{\rho_{ref}^*\sqrt{T^*}\,d_p^*}{\mu_{ref}^*}$$

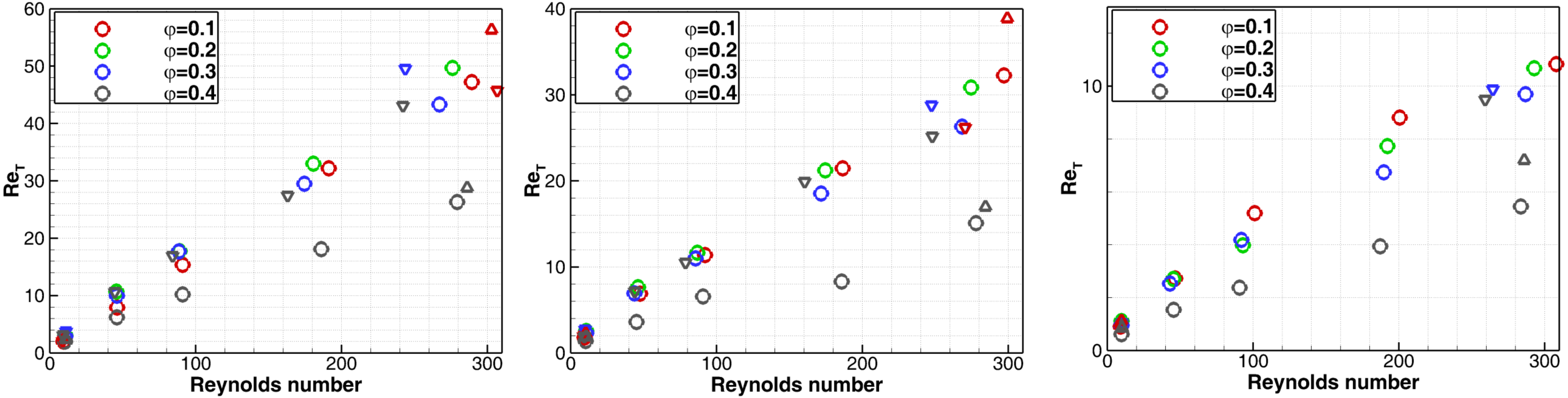

$\frac{\rho_s}{\rho_f} = 2$ $\frac{\rho_s}{\rho_f} = 10$ $\frac{\rho_s}{\rho_f} = 100$

- Considering the case at $\varphi = 0.4$, increase in grid resolution increases the particle velocity fluctuation, whereas the increase in domain size doesn't have much effect on the particle mobility, this might be the reason why results from $9 \times 9 \times 9$ domain has negligible deviation from the results in $5 \times 5 \times 5$ domain.

Conclusion

- Increased domain size from $5 \times 5 \times 5$ to $9 \times 9 \times 9$ doesn't affect the suspension averaged drag force;
- Increased grid resolution from $\frac{1}{40}d_{eq}$ to $\frac{1}{80}d_{eq}$ enhances the drag in particle suspensions with $\varphi = 0.4$;
- The increase of drag results from the enhanced particle mobility;
- Tavanashad's correlation agrees with current PRS data well at $\varphi \leq 0.3$; whereas Huang's correlation reasonably captures the variation of drag from domains using dfferent grid resolutions at $\varphi = 0.4$.